

See discussions, stats, and author profiles for this publication at: <https://www.researchgate.net/publication/293045500>

Experimental analysis of the fitting error of diffractive liquid crystal wavefront correctors for atmospheric turbulence...

Article in *Optics Communications* · May 2016

DOI: 10.1016/j.optcom.2016.01.038

CITATIONS

0

READS

42

8 authors, including:



Zhaoliang Cao

74 PUBLICATIONS 448 CITATIONS

[SEE PROFILE](#)



Quanquan Mu

Chinese Academy of Sciences

124 PUBLICATIONS 738 CITATIONS

[SEE PROFILE](#)



Lishuang Yao

Chinese Academy of Sciences

43 PUBLICATIONS 128 CITATIONS

[SEE PROFILE](#)



Lifa hu

Jiangnan University

130 PUBLICATIONS 771 CITATIONS

[SEE PROFILE](#)

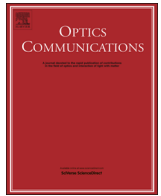
Some of the authors of this publication are also working on these related projects:



Imaging the neural mechanisms of TMS neglect-like bias [View project](#)



adaptive optics application; Liquid Crystal optical modulator design. [View project](#)



Experimental analysis of the fitting error of diffractive liquid crystal wavefront correctors for atmospheric turbulence corrections

Lina Shao^{a,b}, Zhaoliang Cao^{a,*}, Quanquan Mu^a, Peiguang Zhang^a, Lishuang Yao^a, Shaoxin Wang^a, Lifa Hu^a, Li Xuan^a

^a State Key Laboratory of Applied Optics, Changchun Institute of Optics, Fine Mechanics and Physics, Chinese Academy of Sciences, Changchun, Jilin 130033, China

^b University of Chinese Academy of Sciences, Beijing 100049, China

ARTICLE INFO

Article history:

Received 1 October 2015

Received in revised form

10 December 2015

Accepted 14 January 2016

Available online 4 February 2016

Keywords:

Adaptive optics

Liquid-crystal device

Atmospheric correction

Fitting error

ABSTRACT

An experimental analysis was conducted to investigate the fitting error of diffractive liquid crystal wavefront correctors (LCWFCs). First, an experiment was performed to validate the theoretical equations presented in our previous work Cao et al., 2009 [9]. The results showed an apparent discrepancy between the theoretical and measured results for the fitting error. This difference was examined and the influence of nonlinearities and rounding errors generated by the LCWFC was analyzed and discussed. Finally, the fitting error formula of the LCWFC was modified to obtain a more effective tool for the design of LCWFCs for atmospheric turbulence correction. These results will be useful for researchers who design liquid crystal adaptive optics systems for large-aperture ground-based telescopes.

© 2016 Elsevier B.V. All rights reserved.

1. Introduction

Liquid crystal adaptive optics has been widely investigated [1–4]. Although the monochromatic nature of the liquid crystal wavefront corrector (LCWFC) makes it useful only for a very restricted number of cases on large telescopes, it is still a very potential solution to correct for atmospheric turbulence in large-aperture telescopes [5–7] because of its advantages, including millions of pixels, compact size, and low price. To correct for atmospheric turbulence, the fitting error will be produced by the discrete actuators of the wavefront correctors (WFCs) as described by Hudgin [8], who has published a formula to calculate the fitting error for deformable mirrors. It must be noted, however, that we have previously demonstrated (Cao et al., 2009, [9]) that Hudgin's method is not suitable for diffractive WFCs. Normally, the kinoform method [10,11] is utilized to produce a large phase magnitude for LCWFCs. To implement the kinoform technique, the phase modulation is wrapped into 1λ and then quantized with the corresponding LC pixels. Therefore, the quantization level means the number of LC pixels needed to realize 1λ phase modulation. Because the pixel size of LCWFC is on the order of microns, the wavefront fitting error is directly determined by the quantization level without the need to consider the pixel size. Its diffracted wavefront root mean square (RMS) error is [12]:

$$\varepsilon = \frac{\lambda}{2\sqrt{3}N} \quad (1)$$

where λ is the wavelength and N is the quantization level. To calculate the fitting error of the LCWFC, the quantization level N should be calculated first. We have previously developed a formula to calculate N as follows [9]:

$$P = 6.25N + (15 - 1.5D - 23N + 0.91ND)r_0^{-5/6} \quad (2)$$

where P is the pixel number of the LCWFC along one dimension, D is the telescope aperture, and r_0 is the atmospheric coherence length. The units of D and r_0 are centimeters. Here N is defined as the minimum quantization level that meets the condition that the sum of the quantization levels larger than N should occupy 95% of the quantization levels included in the atmospheric turbulence. The quantization level N can be calculated if D , r_0 , and P are constant. Then, the fitting error can be obtained with Eq. (1). In other words, when the telescope aperture and the atmospheric turbulence coherence length are known, the LCWFC can be designed by using Eqs. (1) and (2).

In our former work, the fitting error of the LCWFC is only theoretical analyzed and simulated [9]. In the paper, experimental analysis on the fitting error of the LCWFC will be performed and the actual characteristics of the LCWFC, such as the nonlinear phase modulation and the quantization step error will be considered. Firstly, the validation experiment is performed. Then, the performances of LCWFC are considered and its effects on the

* Corresponding author.

E-mail address: caozlok@ciomp.ac.cn (Z. Cao).

fitting error are analyzed. At last, a modified equation is given.

2. Validation experiment

2.1. Validation scheme

To validate the fitting error formulas of the LCWFC, a comparison must be performed between the theoretical and experimental fitting errors. To measure the fitting error of the LCWFC, the atmospheric turbulence wavefront $\phi(P, D, r_0)$ should first be calculated from Kolmogorov turbulence theory [13,14]. Then, the calculated atmospheric turbulence wavefront is sent to the LCWFC and reproduced by it. Finally, the reproduced wavefront $\phi_m(P, D, r_0)$ is measured. With the calculated and measured atmospheric turbulence wavefronts, the RMS value of the fitting error can be computed by:

$$\varepsilon_{\text{exp}} = \sqrt{\langle |\phi_m(P, D, r_0) - \phi(P, D, r_0)|^2 \rangle} \quad (3)$$

where $\langle |\cdot|^2 \rangle$ denotes phase variance.

The atmospheric turbulence wavefront is described with Noll's Zernike polynomials model [13]. The first 406 modes of the Zernike polynomials are used to simulate the atmospheric turbulence wavefront. To produce the fitting wavefront with the kinoform technique, the simulated atmospheric turbulence wavefront shown in Fig. 1(a) should be wrapped into 1λ and quantified. Then, the quantified wavefront is converted to a gray map for driving the LCWFC as shown in Fig. 1(b).

A parallel-aligned LCWFC (BNS, P256) was used to produce the atmospheric turbulence wavefront with a $6.14 \times 6.14 \text{ mm}^2$ aperture, 256×256 pixels, and $24 \mu\text{m}$ pixel pitch. The previous calculated results [9] showed that the quantization level $N \geq 8$ is suitable for the wavefront correction. Hence, this level was selected to perform the fitting error evaluation. To evaluate the fitting error of the LCWFC, different conditions were considered with the atmospheric coherence length of 10 cm and the selected parameters are shown in Table 1. Using these parameters, the theoretical fitting error ε_T can be calculated as shown in Table 1.

2.2. Optical layout

A Fizeau interferometer (ZYGO) was used to measure the reproduced wavefront of the LCWFC; its optical layout is shown in

Table 1

Selected parameters and the theoretical fitting errors.

N	P	D/r_0	$D(\text{m})$ ($r_0=10 \text{ cm}$)	$\varepsilon_T(\lambda)$
8	64	6	0.6	0.0361
9	100	13	1.3	0.0321
10	128	16.9	1.69	0.0289
11	128	14.1	1.41	0.0262
12	128	11	1.1	0.0241
13	256	31	3.1	0.0222
14	256	28	2.8	0.0206

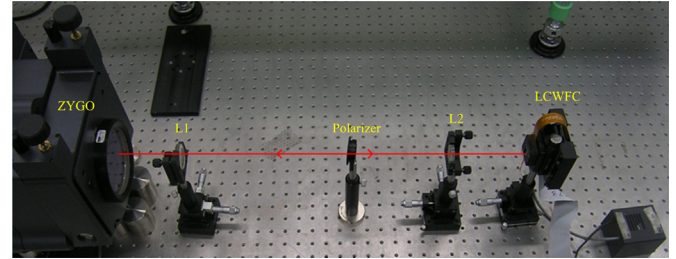


Fig. 2. Optical layout for measuring the reproduced wavefront.

Fig. 2. The combination of lenses L1 and L2 is used to amplify the sampling area of the ZYGO interferometer. A polarizer is utilized to make the polarization direction of the light parallel to the alignment direction of the LC molecules. The collimating laser beam emitted from ZYGO interferometer passes through two lenses and a polarizer, and then it is reflected by the LCWFC. The reflected light enters the ZYGO interferometer and the reproduced wavefront of the LCWFC can then be measured.

2.3. Experimental result

As the atmospheric turbulence is random, 100 atmospheric turbulence wavefronts were utilized to calculate the fitting error according to Eq. (3). Before measuring the reproduction wavefront, the reference wavefront should be measured to eliminate the distortion caused by optical aberration. The fitting error formula of Eq. (3) can be rewritten as:

$$\langle \varepsilon_{\text{exp}} \rangle = \sqrt{\langle |\phi_m - \phi_{\text{ref}} - \phi|^2 \rangle} \quad (4)$$

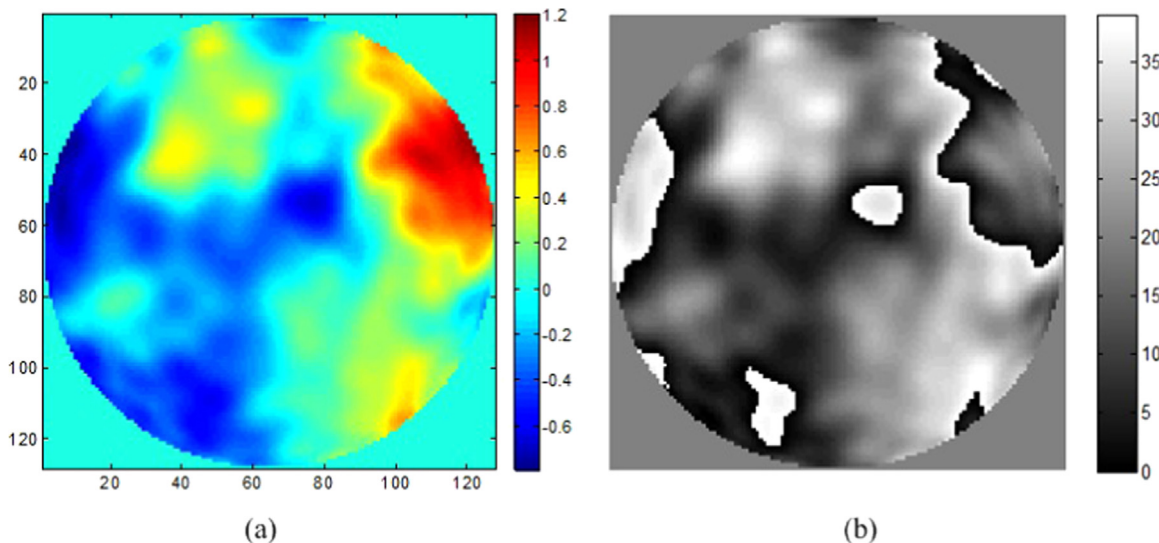


Fig. 1. Atmospheric turbulence wavefronts: (a) Simulated; (b) Gray map.

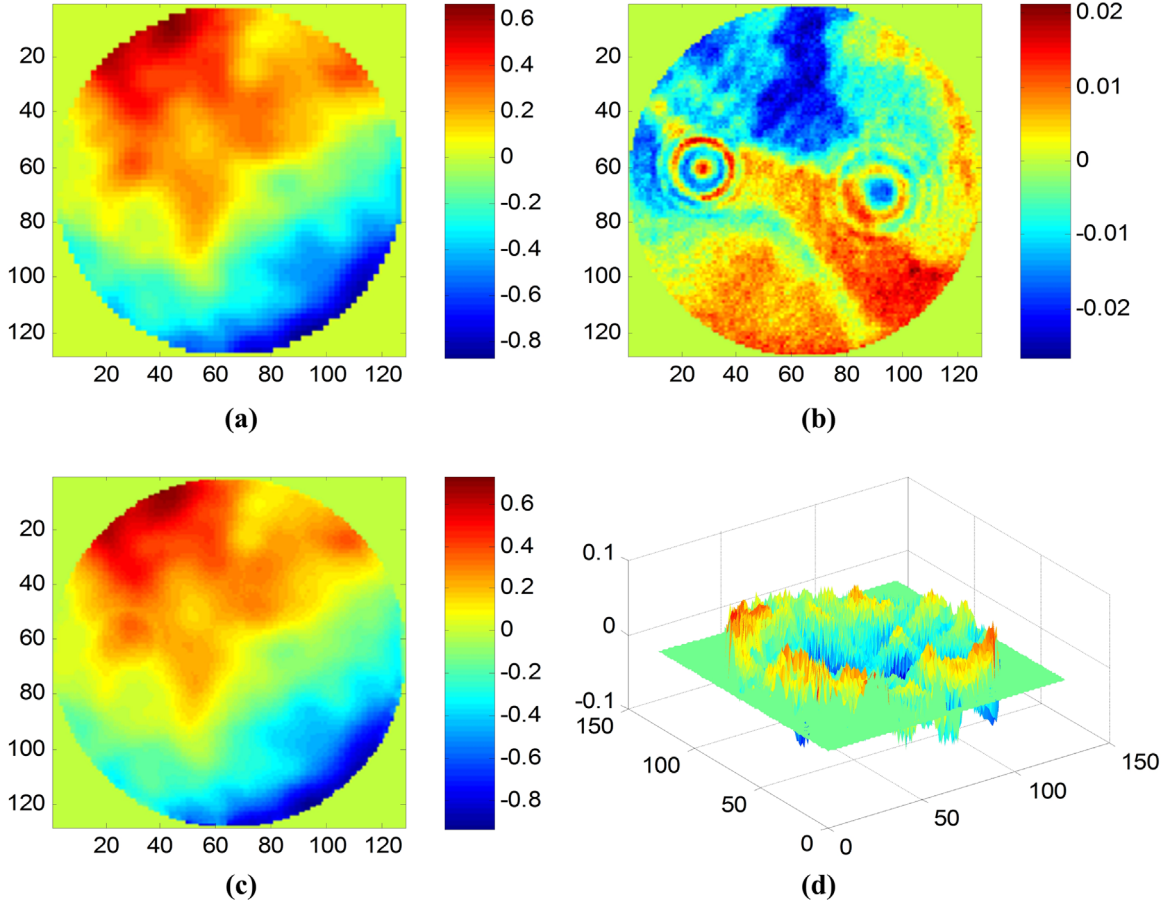


Fig. 3. Atmospheric turbulence wavefronts: (a) Original; (b) Reference; (c) Measured; (d) Residual.

where $\langle \varepsilon_{exp} \rangle$ denotes the statistic average value, and ϕ_{ref} represents the reference wavefront.

Fig. 3 shows the simulated, reference, measured, and residual wavefronts for $N=10$. It can be seen that the reproduced wavefront is very close to the simulated wavefront and the residual RMS value is 0.024λ . Based on Eq. (4), the statistical average value of the fitting wavefront error is computed for different quantization levels; the calculated results are shown in Fig. 4; the solid squares (■) represent the theoretical result that was calculated with Eq. (1) and the solid circles (●) represent the experimental

result that was computed with Eq. (4). It is obvious that the shape of the two curves is almost the same; however, there is an offset difference between two curves. We believe that the offset is caused by errors that will be analyzed in the next section.

3. Error analysis

In our previous work [9], the LCWFC was considered an ideal device, but in reality, the LCWFC can produce a phase-step error that is caused by the phase nonlinearity and the finite number of gray levels.

3.1. Effect of phase modulation nonlinearity

The LCWFC is very similar to a liquid crystal display (LCD). Hence, the LCWFC panel is driven by the gray level map, and each gray level corresponds to a different voltage. The LCWFC used in this study has an 8-bit gray level (0–255), but only half of the levels (128–255) are used to drive the LCWFC. The phase modulation as a function of gray level is shown in Fig. 5(a), and the relationship curve is clearly nonlinear. However, the relation between the phase modulation and the gray level must be linear in order to perform an accurate waveform correction. To achieve this, a Gamma correction technique was selected that has been widely used with LCDs to correct the nonlinearity between the brightness and the voltage [15]. When we send the gray map to the LCWFC, it is first converted with a look-up table (LUT) as shown in Fig. 5(b), and then the converted gray map is utilized to drive the LCWFC [16]. The function of the LUT is to create a linear relationship between the phase modulation and the gray level. By using the LUT,

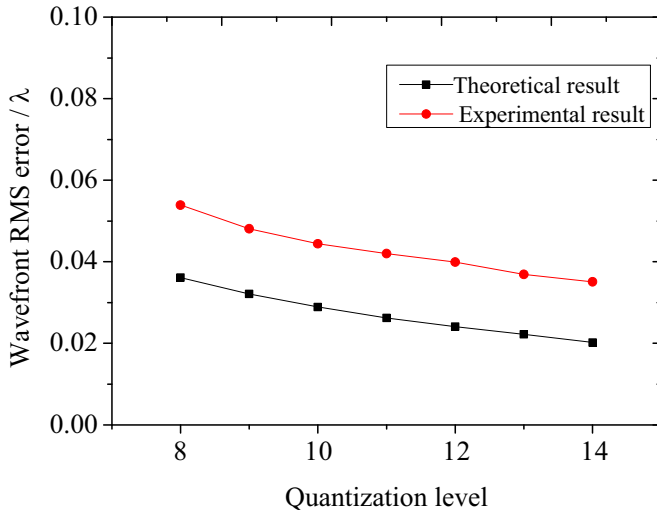


Fig. 4. Wavefront fitting error as a function of the quantization level.

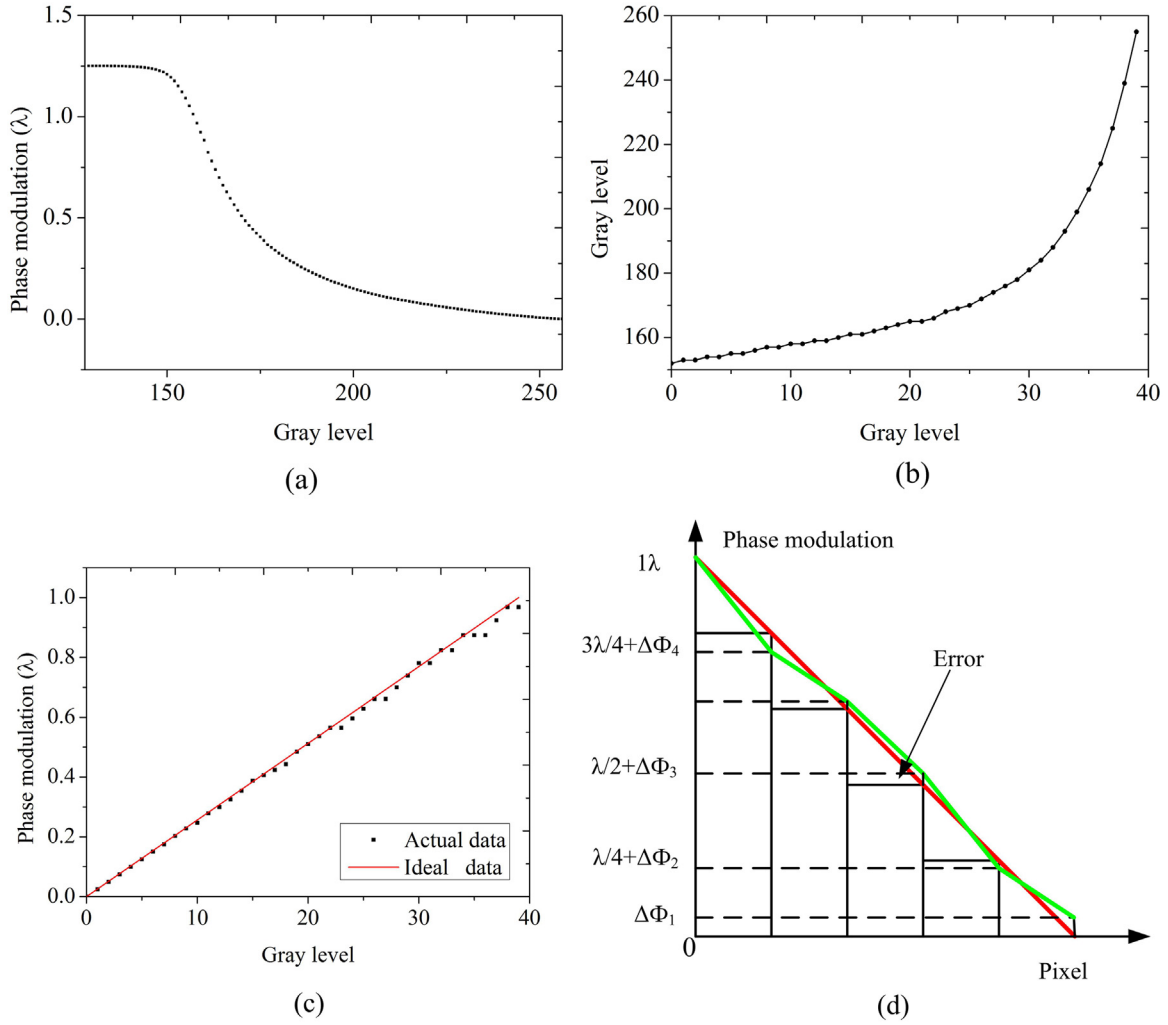


Fig. 5. Effect of the phase modulation nonlinearity: (a) Nonlinear phase modulation; (b) LUT; (c) Linearized phase modulation; (d) Influence of minor nonlinearity on the phase step.

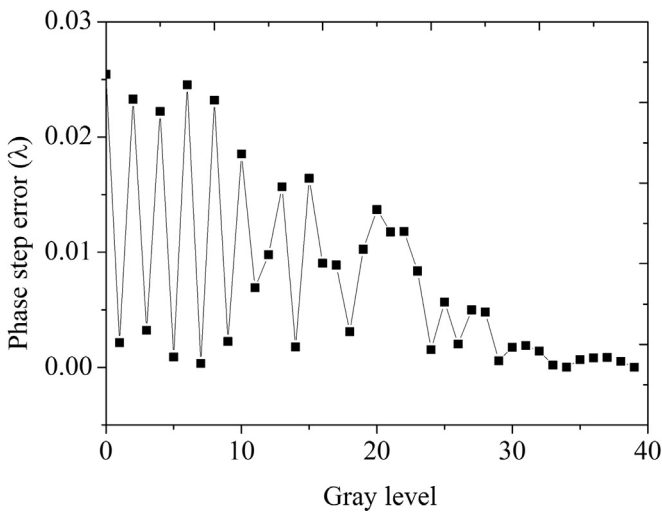


Fig. 6. Phase-step error at each gray level.

the linearized phase modulation curve with 40 gray levels was produced, as shown in Fig. 5(c). The dots are the actual linearized data and the line is the ideal curve. It can be seen that, even after the linearization, the minor nonlinearities still exist and deviation

occurs for some gray levels. These minor deviations will cause height errors of the phase step as shown in Fig. 5(d), and the fitting error of the LCWFC will be increased. To analyze the effect of the minor nonlinearities, the difference between the ideal and the actual phase magnitude is first calculated as shown in Fig. 6. This phase magnitude error may be expressed as

$$\delta_1(j) = |P_{ideal} - P_{actual}| \quad (5)$$

where P_{ideal} represents the ideal phase modulation and P_{actual} represents the actual phase modulation.

As the wavefront-fitting error caused by each gray level is independent, the total effect of the nonlinear errors may be computed by

$$\varepsilon_1 = \sqrt{\frac{\lambda^2}{M} \sum_{m=1}^M \delta_1^2(m)} \quad (6)$$

where M is the number of gray levels. The calculated results show that the fitting RMS error of the phase nonlinearity is 0.0118λ .

3.2. Effect of finite gray levels

The number of gray levels is 40 for the LCWFC. As the LCWFC only produces 1λ of phase modulation, the accuracy of the phase step is $\lambda/39$. Hence, the fact that the number of gray levels is finite will cause fitting errors.

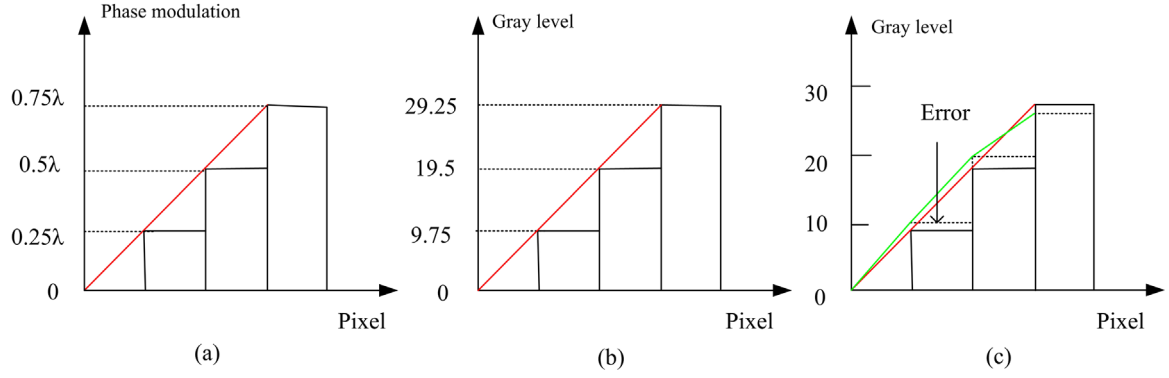


Fig. 7. Influence of rounding error on phase distribution: (a) Quantization with four levels; (b) Transformed gray levels with $M=40$; (c) phase-step errors caused by rounding.

The kinoform gray map of the simulated atmospheric turbulence wavefront is calculated by

$$\Phi_{\text{grey}} = \text{round}((\text{mod}(\Phi_{\text{tur}}, 1)) \times (M - 1)) \quad (7)$$

where $\text{mod}()$ denotes the modulus of the wavelength and $\text{round}()$ represents rounding to the nearest integer. Fig. 7 shows an example of the quantization with 4 levels. 1λ is quantified as shown in Fig. 7(a). As $M=40$, other gray levels are not integers as shown in Fig. 7(b). Fig. 7(c) is the rounded result of Fig. 7(b). It can be seen that a phase-step height error is produced that will affect the fitting accuracy of the LCWFC.

According to Eq. (7), the range of gray level rounding errors is $[-1/2, 1/2]$. When the number of gray levels equals M , the phase-step error δ_2 caused by the rounding is $[-\lambda/2(M-1), \lambda/2(M-1)]$. Because the rounding-off integers rule is an equal probability event, the phase-step error δ_2 may be considered as an equal probability distribution and its probability density function (PDF) $f(\delta_2)$ is illustrated in Fig. 8. Based on the definition of PDF [17], the following equation may be obtained

$$\int_{-\frac{\lambda}{2(M-1)}}^{\frac{\lambda}{2(M-1)}} f(\delta_2) d\delta_2 = 1 \quad (8)$$

By integrating Eq. (8), $f(\delta_2)$ equals $(M-1)/\lambda$, and the mean square of the phase-step error may be written as

$$\varepsilon_2^2 = \int_{-\frac{\lambda}{2(M-1)}}^{\frac{\lambda}{2(M-1)}} f(\delta_2) \delta_2^2 d\delta_2 = \frac{\lambda^2}{12(M-1)^2} \quad (9)$$

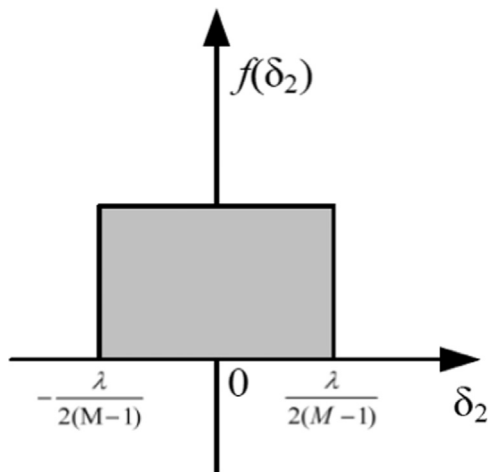


Fig. 8. Equal probability distribution of the phase-step error.

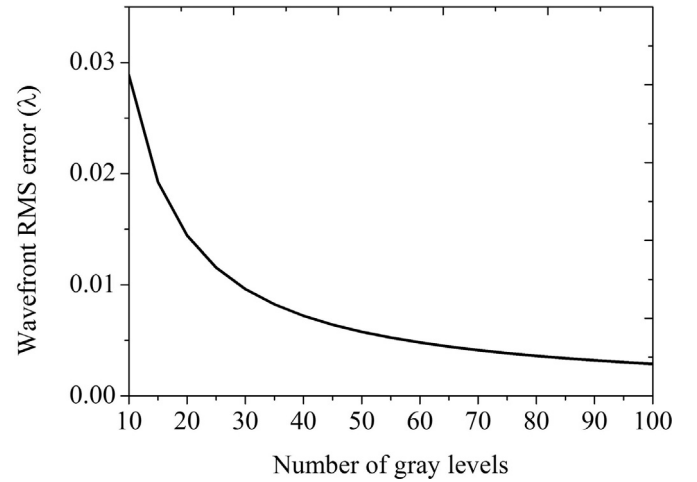


Fig. 9. The rounding error as a function of the number of gray levels.

Thus the wavefront RMS error caused by the rounding is

$$\varepsilon_2 = \frac{\lambda}{2\sqrt{3}(M-1)} \quad (10)$$

The wavefront error caused by the rounding is shown in Fig. 9; with the increase of the gray levels, the wavefront error drops drastically at first, and then gradually approaches to zero. For $M=40$, the wavefront RMS error is 0.0074λ .

3.3. Fitting error equation modification

From the above error analysis, we can see that these errors should be subtracted from the experimental results to evaluate the theoretical fitting error equations. The minor nonlinearity error and rounding error are both related to the number of gray levels, thus the contributions of these two errors are statistically dependent, and the experimental fitting error may be calculated by:

$$\varepsilon'_{\text{exp}}{}^2 = \varepsilon_{\text{exp}}{}^2 - (\varepsilon_1^2 + \varepsilon_2^2) \quad (11)$$

After eliminating the error, the experimental and theoretical fitting error curves are as shown in Fig. 10. It is obvious that the experimental result is very close to the theoretical result. The difference is small: about 0.013λ . Consequently, the experimental results validate the theoretical equations for the fitting error of the diffractive LCWFCs.

For the actual applications of the LCWFC on a large-aperture telescope, these errors must be considered, and then the

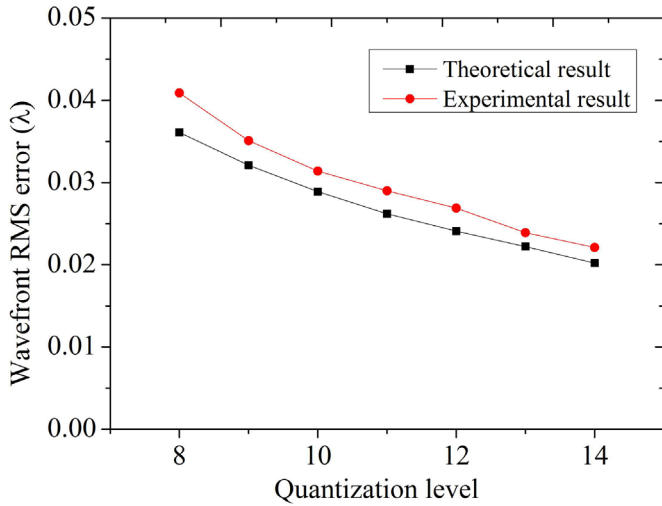


Fig. 10. Relation between the wavefront error and the quantization level after elimination of the device error.

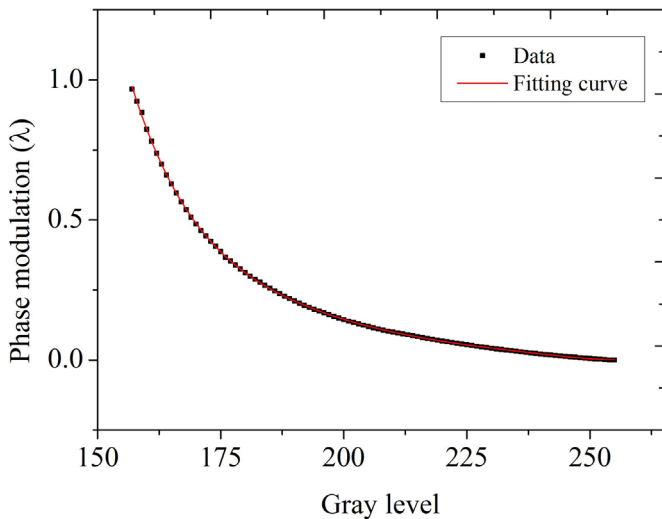


Fig. 11. 1λ phase data and its fitting curve.

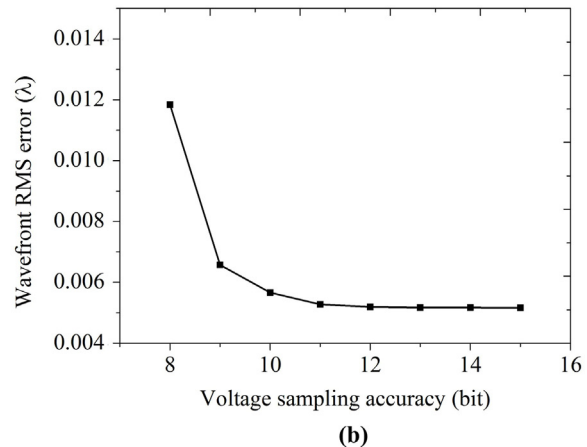
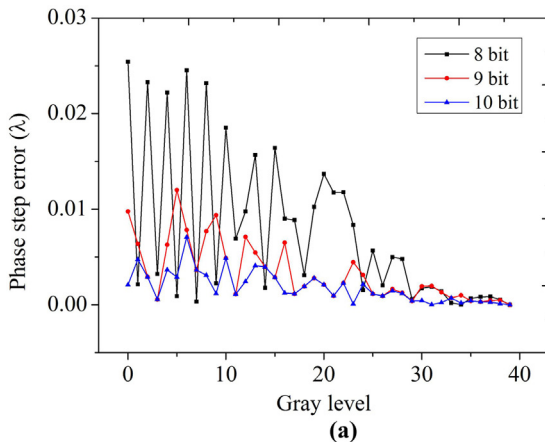


Fig. 12. Effects of the driving voltage sampling accuracy on the wavefront: (a) Phase-step error; (b) Wavefront error as a function of voltage sampling accuracy.

theoretical equation Eq. (1) should be modified as

$$\varepsilon^2 = \left(\frac{\lambda}{2\sqrt{3}N} \right)^2 + \frac{\lambda^2}{M} \sum_{m=1}^M \delta_1^2(m) + \left(\frac{\lambda}{2\sqrt{3}(M-1)} \right)^2 \quad (12)$$

Seen from the Eq. (12), the fitting error of the diffractive LCWFC is composed of three main terms: the first term is the quantization error caused by kinoform technology; the second term is the nonlinear error caused by phase linearization; the third term is the rounding error caused by the finite gray levels of the graph.

Normally, after the phase is linearized, the gray levels of the LCWFC will be greater than 30. With $M=30$, the wavefront RMS error is as small as $\lambda/100$. Therefore, the rounding error has a minor effect on the fitting error which can be neglected. However, the nonlinear error is slightly larger from the above analysis. In the following discussion, we will mainly consider the effect of the phase nonlinearity.

As shown in Fig. 5(c), we can see that, because only 40 gray levels can be chosen with the sample resolution of 8 bits, a minor nonlinearity still exists. To decrease the minor nonlinearity error, a higher sample resolution is needed so that we can select more gray levels. Consequently, the nonlinear phase modulation curve should be sampled at more than 8 bits. To investigate the effect of sample resolution on the phase nonlinearity, 1λ phase modulation of the LCWFC should first be chosen from Fig. 5(a), and then fitted to an exponential function as shown Fig. 11. With this fitted curve, an arbitrary sample resolution can be produced and the simulation analysis can be performed. The fitting curve may be expressed as

$$y = \exp(7.059 - 0.046x) \quad (13)$$

where x is the gray level. By using Eq. (13), the discrete phase modulation value can be acquired for an arbitrary sample resolution. Consequently, the wavefront error caused by the phase nonlinearity may be calculated for different voltage sampling accuracies as shown in Fig. 12. The phase-step error is shown in Fig. 12(a) for 8, 9, and 10 bits respectively. It can be seen that the phase-step error is decreased by improving the voltage sampling accuracy. According to the calculated phase-step error, the wavefront error can be computed by using Eq. (6); the results are shown in Fig. 12(b): As the voltage sampling accuracy increases, the wavefront error falls rapidly at first, and then gradually approaches zero. Furthermore, the wavefront RMS error is as small as $\lambda/100$ for 9 bits. Therefore, to eliminate the effect of the phase nonlinearity, the sample accuracy of the LCWFC should be more than 9 bits.

4. Conclusions

The fitting error of diffractive LCWFCs has been considered for actual applications. To validate the theoretical results of our former work [9], a validation experiment was performed. The experiment showed that the measured wavefront fitting error was larger than that of the theory by 0.021λ even though the shape of its functional dependence was similar to the theoretical results. To explain this difference, the nonlinearities and rounding errors of the LCWFC were analyzed and discussed.

First, the equations were established to calculate the nonlinear and rounding errors. Then, according to the parameters of the LCWFC, the effects of the nonlinear and rounding errors on the fitting wavefront were computed and eliminated from the measured results. It was shown that, by subtracting the errors, the experiment results can be brought very close to the theoretical results.

Furthermore, a modified equation for the fitting error was developed. The modified fitting error equation is composed of three main terms: the quantization error caused by kinoform technology; the nonlinear error caused by phase linearization; and the rounding error caused by the finite gray levels of the graph. Each of the error terms is added in quadrature to yield a total value for the fitting error of the diffractive LCWFC. The effects of each error term on the total fitting error of the LCWFC were discussed in detail. We conclude that, to design a better LCWFC for atmospheric turbulence correction, the linearized gray levels and the driving voltage sampling accuracy should be more than 30 levels and 9 bits respectively. This work demonstrates that, to design an effective liquid crystal adaptive optics system (LC AOS) for a large-aperture telescope, the actual characteristics of the LCWFC must be considered.

In summary, to compensate for atmospheric turbulence effectively, a modified fitting error calculation method has been established for diffractive LCWFCs. The results of this work will be very helpful in designing the LC AOS for large-aperture ground-based telescopes.

Acknowledgments

This work is supported by the National Natural Science Foundation of China (11174274, 11174279).

References

- [1] M.J. Booth, Adaptive optical microscopy: the ongoing quest for a perfect image, *Light-Sci. Appl.* 3 (2014) 1–7.
- [2] D. Dayton, J. Gonglewski, S. Restaino, J. Martin, J. Phillips, M. Hartman, P. Kervin, J. Snodgrass, S. Browne, N. Heimann, M. Shilko, R. Pohle, B. Carrion, C. Smith, D. Thiel, Demonstration of new technology MEMS and liquid crystal adaptive optics on bright astronomical objects and satellites, *Opt. Express* 10 (25) (2002) 1508–1519.
- [3] S. Restaino, D. Dayton, S. Browne, J. Gonglewski, J. Baker, S. Rogers, S. McDermott, J. Gallegos, M. Shilko, On the use of dual frequency nematic material for adaptive optics system: first results of a closed-loop experiment, *Opt. Express* 6 (1) (2000) 2–6.
- [4] K.N. Yao, J.L. Wang, X.Y. Liu, W. Liu, Closed loop adaptive optics system with a single liquid crystal spatial light modulator, *Opt. Express* 22 (14) (2014) 17216–17226.
- [5] Q.Q. Mu, Z.L. Cao, L.F. Hu, Y.G. Liu, Z.H. Peng, L.S. Yao, L. Xuan, Open loop adaptive optics tested on 2.16 m telescope with liquid crystal corrector, *Opt. Commun.* 28 (2012) 896–899.
- [6] G.D. Love, Wavefront correction and production of Zernike modes with a liquid-crystal spatial light modulator, *Appl. Opt.* 36 (7) (1997) 1517–1520.
- [7] G.D. Love, Liquid crystal adaptive optics, in: R.K. Tyson (Ed.), *Adaptive Optics Engineering Hand Book*, CRC, Boca Raton, 1999.
- [8] R. Hudgin, Wavefront compensation error due to finite corrector-element size, *J. Opt. Am.* 67 (3) (1977) 393–395.
- [9] Z.L. Cao, Q.Q. Mu, L.F. Hu, X.H. Lu, L. Xuan, A simple method for evaluating the wavefront compensation error of diffractive liquid-crystal wavefront correctors, *Opt. Express* 17 (20) (2009) 17715–17722.
- [10] A. Tanone, Z. Zhang, C.M. Uang, F.T.S. Yu, D.A. Gregory, Phase modulation depth for a real-time kinoform using a liquid crystal television, *Opt. Eng.* 32 (3) (1993) 517–521.
- [11] J. Amako, T. Sonehara, Kinoform using an electrically controlled birefringent liquid-crystal spatial light modulation, *Appl. Opt.* 30 (32) (1991) 4622–4628.
- [12] M.A. Golub, I.N. Sisakian, V.A. Soifer, Phase quantization and discretization in diffractive optics, *Proc. SPIE* 1334 (1990) 188–199.
- [13] R.J. Noll, Zernike polynomials and atmospheric turbulence, *J. Opt. Soc. Am.* 66 (3) (1976) 207–211.
- [14] N. Roddier, Atmospheric wavefront simulation using Zernike polynomials, *Opt. Eng.* 29 (10) (1990) 1174–1180.
- [15] K. Xiao, C. Fu, D. Karatzas, S. Wuergler, Visual gamma correction for LCD displays, *Displays* 32 (2011) 17–23.
- [16] Z.L. Cao, Q.Q. Mu, G. Dovillaire, T. Grandin, L.F. Hu, L. Xuan, Effect of the twisted alignment on the liquid crystal wavefront corrector, *Liquid Cryst.* 34 (10) (2007) 1227–1232.
- [17] J.L. Devore, *Probability and Statistics for Engineering and the Sciences*, California Polytechnic State University Press, San Luis Obispo, 2010.